Investigating the role of BN-domains of FlhF involved in flagellar synthesis in *Campylobacter jejuni*

Xiaofei Li[a], Qinwen Chai[a], Lina Zheng[b], Pingyu Huang[b], Ozan Gundogdu[d], Xinan Jiao[c], Yuanyue Tang[c*], Jinlin Huang[c*]

[a]Jiangsu Key Laboratory of Zoonosis, Jiangsu Co-Innovation Center for Prevention and Control of Important Animal Infectious Diseases and Zoonoses, Yangzhou University, Yangzhou, Jiangsu 225009, China

[b]Key Laboratory of Prevention and Control of Biological Hazard Factors (Animal Origin) for Agrifood Safety and Quality, Ministry of Agriculture of China, Yangzhou, Jiangsu 225009, China

[c]Joint International Research Laboratory of Agriculture and Agri-product Safety, Ministry of Education of China, Yangzhou, Jiangsu 225009, China

[d] Department of Infection Biology, Faculty of Infectious & Tropical Diseases, London School of Hygiene &Tropical Medicine, Keppel Street, London WC1E 7HT, UK.

*Correspondence: Yuanyue Tang, tangyy@yzu.edu.cn; Jinlin Huang, jinlin@yzu.edu.cn

Abstract:

FlhF protein is critical for intact flagellar assembly in *Campylobacter jejuni*. It is a putative GTPase with B-, N- and G-domains. However, the role of the B- and N-domains in flagella biosynthesis remains unclear in *C. jejuni*. This study demonstrated that both the B- and N-domains are essential for flagellar synthesis, with the absence of B- and/or N-domains showing truncated variants of FlhF by TEM. Point mutations in the B- and N-domains (T13A, K159A, G231A) also induced flagella abnormalities. Furthermore, significant defects in GTPase activity and polar targeting of FlhF were triggered by point mutations of B- and N-domains. Flagella gene expression and transcription were also significantly disrupted in *flhF*(T13A), *flhF*(K159A) and *flhF*(G231A) strains. This study initially explored the effects of B- and N-domains on flagella synthesis. We speculated that B- and N-domains may directly or indirectly cause flagella abnormalities by affecting flagellar gene expression or GTPase activity, which helps us better understand the function of FlhF in flagella synthesis.

Keywords: *Campylobacter jejuni*; FlhF; flagellar synthesis; B-domain; N-domain

1. Introduction

FlhF is described as a putative GTP binding protein containing B-, N- and G-domains (Bange et al., 2007; Mazzantini et al., 2020; Schuhmacher et al., 2015; Terashima et al., 2020). These three domains are essential for the function of FlhF. The G-domain with GTPase activity predominantly affects the location and number of flagella synthesis (Balaban et al., 2009; De Nisco et al., 2018). However, the role of the B- and N-domains remain unclear. In *Bacillus subtilis*, the B-domain regulates and stabilizes the dimer,

thereby better binding to GTP (Bange et al., 2007). The N-domain rearranges the signal recognition particle (SRP) conformation when the ribosome is bound to stabilize the GTP binding state (Halic et al., 2006). In *Vibrio cholerae*, the N-domain determines the polar positioning of the flagella, while the B-domain participates in the recruitment of FliF, a component of the flagellar MS-ring to the cell pole (Green et al., 2009; Schniederberend et al., 2013). However, in *C. jejuni*, the roles of B-domain and N-domains have not been elucidated, specifically in relation to FlhF and in flagella synthesis.

In bacteria with polar flagellar, the synthesis mechanism of flagella has been the object of research for many years (Ferreira et al., 2021; Gao et al., 2015). FlhF is a key protein affecting flagella biosynthesis (Kojima et al., 2020; Mazzantini et al., 2020; Zhang et al., 2020). In many species, the inactivation of *flhF* leads to a series of abnormal flagella phenotypes (Burnham & Hendrixson, 2018; Kazmierczak & Hendrixson, 2013). In *C. jejuni*, motility and flagella are completely abolished without *flhF* (Li et al., 2020). Although the effect of FlhF on flagella assembly has been widely studied, the regulatory mechanism of flagellar synthesis is still unclear (Terashima et al., 2020).

Among the three domains of FlhF, the influence of G-domain with GTPase activity has been widely reported (Balaban et al., 2009; Bange et al., 2007; De Nisco et al., 2018). Mutations within G-domain of *flhF* in *Vibrio alginolyticus* reduce polar localization (Kondo et al., 2017). In *Shewanella* spp., the GTPase activity of FlhF is critical for bacterial motility, not for the location of flagella (Gao et al., 2015). In *V. cholerae,* the polar localization of FlhF is independent of its GTPase activity (Green et al., 2009).

In *C. jejuni*, *flhF* mutants without GTPase activity cause ectopic flagella synthesis, and the interaction between FlhG and FlhF may mechanistically contribute to flagellar number variation (Arroyo-Perez & Ringgaard, 2021; Gulbronson et al., 2016; Schuhmacher et al., 2015). These observations also indicate that the function of FlhF domain may vary depending on the bacterial species.

This study is aimed to elucidated the roles of the B- and N-domain involved in flagellar synthesis and gene expression in *C. jejuni*. Transmission Electron Microscope (TEM) visualization and motility assays were performed to evaluate the influence of B- and N-domain of FlhF on flagellar synthesis. We investigated flagella assembly and gene expression functionality of B- and N- domains using point mutants of *flhF* BN-domains with GTPase activity in conjunction with transcriptional and translational analysis. The findings in this study helps us better understand the FlhF protein's function in flagella synthesis in *C. jejuni*.

2. Material and methods

2.1 Bacterial strains and plasmids

The strains and plasmids used in this study are listed in Table S1. *C. jejuni* strains were inoculated on *Campylobacter* blood-free selective agar containing charcoal cefoperazone deoxycholate (CCDA) (Oxoid, Basingstoke, UK), and incubated under microaerobic conditions at 42°C. *Escherichia coli* strains were grown in Luria-Bertani (LB) broth or on LB agar at 37°C (Li et al., 2020). As required, kanamycin or chloramphenicol was added to the final concentration of 50 μg/mL or 20 μg/mL. The pUOA18 was a *C. jejuni* shuttle vector provided by Qijing Zhang (Iowa State University,

Ames, USA) for triparental mating conjugation, and pCJC4-*gfp* plasmid was previously constructed by Dennis Linton and provided by Ozan Gundogdu (LSHTM, London, UK) (Gundogdu et al., 2011; Jervis et al., 2015).

2.2 Truncation variants of *flhF*, site-directed mutagenesis and GFP fusion construction

flhF mutant strain and complemented strain have been constructed in previous studies. Truncated variants of *flhF* were constructed by complimenting the variant of B-, N-, G-domain on the shuttle vector pUOA18, then using triparental mating with pRK2013 (Biomedal, Beijing, China) as the helper strain. The recombinant plasmid for truncated variants were transferred to the *flhF* null strain as previously described (Li et al., 2020). All primers used for constructing truncated variants were listed in Table S2. Site-directed mutagenesis of the B- and N-domains was constructed by overlap extension PCR, in which candidate amino acids were replaced by alanine (Gao et al., 2015). All target genes were amplified and directly inserted in the shuttle vector pUOA18, and transferred in *flhF* mutant strain by triparental mating.

For GFP fusion construction, *flhF* gene or site-directed mutagenesis were amplified and inserted between the *gfp* gene and the chloramphenicol gene *cat* in the pCJC4-*gfp* vector as described previously (Gundogdu et al., 2016). Briefly, the unique MluI site was introduced between the *gfp* gene and chloramphenicol gene *cat* in the pCJC4-*gfp* vector by inverse PCR mutagenesis (IPCRM). *flhF* gene or site-directed mutagenesis was ligated into the unique MluI site within pCJC4-*gfp*. These constructs were electroporated into the *flhF* mutant strain and putative clones were verified by PCR and sequencing. Primers used for strain construction are listed in Table S2.

106 2.3 Motility assays and transmission electron microscopy

107 Motility assay was conducted on wild-type strain, *flhF* truncated variants, and point
108 mutants as previously described (Ren et al., 2018). Briefly, overnight cultures on CCDA
109 plates were diluted with Mueller-Hinton (MH) broth (BD, USA) to an OD_{600} of 1.0, and
110 pierced into semi-solid MH agar through a sterilized inoculating needle. The plates
111 were cultured under microaerobic conditions at 42°C for 24 h, and then their motility
112 was evaluated.

113 For flagella phenotype analysis, strains were prepared for transmission electron
114 microscopy (TEM) as previously described (Gulbronson et al., 2016). Briefly, strains
115 were cultured and diluted with phosphate-buffered saline (PBS) to an OD_{600} of 0.5, the
116 bacterial solution (1 mL) was centrifuged and resuspended with 2% (vol/vol)
117 glutaraldehyde solution, then incubated on ice for one hour. Samples stained with 1%
118 (wt/vol) uranyl acetate were visualized with TEM (Tecnai 12; Philips; Netherlands).
119 Different flagella phenotypes were counted from 100 individual cells, and the average
120 of three biological replicates was taken to determine the ratio of different flagella
121 phenotypes.

122 2.4 GTPase activity

123 GTPase activity of FlhF, T13A, K159A and G231A were assessed as described
124 previously (Liang & Connerton, 2018). FlhF and point mutants of FlhF were induced
125 to express in *E. coli* BL21 (DE3) system (TaKaRa, Dalian, China) (Li et al., 2020).
126 Briefly, *flhF* and site-directed mutagenesis of *flhF* genes were amplified and inserted in
127 pET-30a (between *Bam*HI and *Xho*I sites). Then FlhF, FlhF point mutants and the empty

vector control (pET-30a without insert) were purified and extracted using the His Bind Purification Kit (Novagen, EMO Millipore corp, Billerica, MA USA). The GTPase activity of FlhF and point mutants of FlhF was evaluated by ATPase/GTPase activity kit (MAK113; Sigma-Aldrich; Merck KGaA, Darmstadt, Germany) according to the kit instructions. The GTPase activity of the empty vector was used as the negative control.

2.5 RNA isolation and quantitative real-time PCR

Quantitative real-time PCR (qRT-PCR) was applied to evaluate the expression of flagellar-related genes including *fliK*, *flgE*, *flhG*, *flaB* and *flaA*. Briefly, the overnight cultures of wild-type 81-176 and point mutants were diluted by MH broth to OD_{600} 0.07, and incubated under microaerobic conditions at 42°C, 100 rpm for 8 h. RNA was extracted using RNeasy plus mini kit (Qiagen, Hilden, Germany) and cDNA was synthesized by RT reagent kit (TaKaRa, Dalian, China). qRT-PCR was performed via a FastStart Universal SYBR Green Master (ROX) (Roche Diagnostics, Mannheim, Germany) in an ABI PRISM 7500 Real-Time PCR System (Applied Biosystems, Foster City, CA, USA). All primers for qRT-PCR were listed in Table S2. The *glyA* gene was served as an endogenous control.

2.6 Preparation of polyclonal antiserum against *C. jejuni* FlhG, FliK and RpoA

FlhG, FliK and RpoA proteins were expressed as described previously (Li et al., 2020). Briefly, the *flhG* and *rpoA* genes were amplified from *C. jejuni* genome, and cloned into pET-30a (between *Bam*HI and *Xho*I sites), then transformed into *E. coli* BL21 (DE3). The *fliK* was amplified and ligated into pET-28a (between *Nde*I and *Xho*I sites). The

FlhG-His_6, FliK-His_6 and RpoA-His_6 proteins were expressed and purified by the His Bind Purification Kit (Novagen, EMO Millipore corp, Billerica, MA USA).

Purified FlhG-His_6, FliK-His_6 and RpoA-His_6 proteins were repeatedly injected intradermally into 6-week-old female BALB/c mice (VITAL RIVER, Beijing, China) together with an equal volume of Freund's complete adjuvant (Sigma, Darmstadt, Germany) to prepare a polyclonal antiserum. The ten μg purified protein emulsified in Freund's incomplete adjuvant (Sigma, Darmstadt, Germany) was administered every two weeks to strengthen the immune response (Kulshreshtha et al., 2015). The untreated group was injected with PBS instead of protein. Afterward, the blood sample of each treated group was collected from the mice, and sera samples were separated and stored at -20 °C. The specificity of antiserum was identified by western blot. The serum from the PBS-treated group was used as a negative control, which was also verified by Western Blot (Fig. S2).

2.7 Western blotting with grayscale analysis

Protein expression was assessed by Western blotting as previously described (Li et al., 2019; Han et al., 2019). Briefly, equal amounts of the whole-cell lysates (WCL) were separated by SDS-PAGE, and transferred to nitrocellulose filter membranes (7 cm × 5cm), which were blocked with 2% (wt/vol) fat-free dry milk in Tris-buffered saline containing Tween 20 (TBST) buffer for 2 h. Then primary antibodies against - FlhF (1:5000), RpoA (1:5000), FlhG (1:1000), FliK (1:1000) were incubated with membranes for 12 h. Secondary goat anti-mouse IgG (1:1000, Cell Signaling Technology, USA) was further incubated with membranes for one h. Results were

scanned by a gel imaging system (Bio-Rad Laboratories, USA). Grayscales were analyzed by ImageJ software (Han et al., 2019). Relative protein expression was normalized to the wild-type (which was set to 100%).

2.8 Fluorescence microscopy

The location of *flhF in situ* was visualized by fluorescence microscopy. Samples of *C. jejuni* strain 81-176 and *flhF* point mutants for fluorescence microscopy were prepared as described previously (Ren et al., 2018). Briefly, *C. jejuni* GFP fusion was diluted with PBS to an OD_{600} of 0.5, ten μL bacterial solution was dropped on a microscope slide, then glass coverslips treated with poly-1-lysine were used to fix cells. The fluorescence of proteins was observed by a Leica TCS SP8 STED confocal fluorescence microscope (Leica Microsystems, Wetzlar, Germany).

2.9 Statistical analysis

The experiments were conducted at least three times, and data were analyzed using Prism GraphPad software (version 6.01) by Student's *t*-test (*P<0.05, **P<0.01, ***P<0.001).

3. Results

3.1 Influence of B- and N-domains on flagellar synthesis

To explore whether B- and N-domain affect flagellar synthesis, we complemented Δ*flhF* with individual domains alone or in combination including $FlhF^{B}$ (residues 1-78), $FlhF^{N}$ (residues 79-272), $FlhF^{G}$ (residues 283-484), $FlhF^{BN}$ (residues 1-272), $FlhF^{NG}$ (residues 79-484), and $FlhF^{BG}$ (residues 78-272 deleted) (Fig. 1A). We assessed the influence of the B- and N-domains on flagellar synthesis by TEM visualization, and

194 none of the truncated variants complemented the flagella defect in the *ΔflhF* strain (Fig.
195 1B). We also examined effects of *flhF* mutants by motility assay. None of the truncated
196 variants complemented the motility defect in the *ΔflhF* strain (Fig. 1A). Altogether, both
197 the B- and N-domains were essential for flagellar synthesis.
198 3.2 Influence of point mutations in the B- and N-domains on the synthesis of FlhF
199 To further investigate the roles of B- and N-domains in motility and flagellar synthesis,
200 we aligned the protein sequences of FlhF from *C. jejuni*, *B. subtilis*, *P. aeruginosa* and
201 *V. cholerae*. Site-directed mutagenesis of *flhF* were generated including F8, T13 in B-
202 domain, K159, G231 in N-domain, which both F8 and G231 were conserved amino
203 acids in the B- and N-domain, respectively (Fig. 2A). The western blot result showed
204 that the production of FlhF (T13A), FlhF (K159A) and FlhF (G231A) protein were
205 similar to wild-type FlhF. However, the production of FlhF (F8A) protein was
206 approximately 60% reduced than that of wild-type FlhF (Fig. 2B), which made it
207 difficult to explain the results of defects in the flagella phenotype.
208 3.3 Disruption of flagellum assembly by point mutations of BN-domains
209 TEM was performed to explore whether these mutants disrupt flagellar biosynthesis.
210 The expected flagellar biosynthesis phenotype should be the production of unipolar or
211 bipolar flagella. Our results demonstrated that 91% of the wild-type strain produced the
212 normal flagellar phenotype (Fig. 3A-panel a and Table 1). However, no flagella were
213 detected in the *flhF* mutant strain (Fig. 3A-panel b and Table 1). A variety of flagellar
214 phenotypes were observed in *flhF* (T13A) mutant, but only approximately 10%
215 contained the normal flagellar phenotype. 61% of the *flhF* (T13A) mutant did not form

flagella (Fig. 3A-panels c-f and Table 1), while 29% of the *flhF* (T13A) had many abnormal flagellar phenotypes including abnormal flagellar position or number, or the shortened flagellum (Fig. 3A-panels c-f). In the *flhF* (K159A) and *flhF* (G231A) mutants, there were approximately 12% and 15% that produced the normal flagellar phenotype, while 51% and 47% of both mutants did not contain flagella, respectively (Fig. 3A-panels g-l and Table 1). In addition, both *flhF* (K159A) and *flhF* (G231A) mutants showed similar abnormal flagellar biosynthesis phenotypes as *flhF* (T13A) mutant (Fig. 3A-panels g-l). The abnormal flagellar phenotypes indicated that the three residues in BN-domains were essential for normal flagellar biosynthesis.

We further examined effect of BN-domain point mutations by motility assay. Our results demonstrated that all *flhF* variants (F8A, T13A, K159A and G231A) had significantly reduced motility compared to the wild-type (Figure 3B). The decrease in F8A motility was the most significant, where approximately 75% decrease in motility was observed compared to the wild-type (WT) (Fig. 3C).

3.4 Potential regulatory mechanism triggered by BN- domains in flagella synthesis

GTPase activity of FlhF was known to be essential for complete flagellar biosynthesis in *C. jejuni*. Thus, we proposed that single-residue substitutions in the B- and N-domains could disrupt complete flagellar biosynthesis by affecting GTPase activity of FlhF. The result found that the GTPase activity of T13A, K159A and G231A were significantly reduced compared to FlhF (Fig. 4A). Meanwhile, FlhF was known to locate at the cell pole, which could interact with FliF and FlhG to regulate the location and number of the flagellum.

We further fused wild-type *flhF* and *flhF* variants (T13A, K159A, G231A) with *gfp* and expressed them in *flhF* mutants. We found that the fluorescence of *flhF* variants was distributed throughout the cell (Figure S1). The above data indicated that three different point mutants in the B and N domains affect the GTPase activity and polar targeting of FlhF in *C. jejuni.*

Furthermore, considering the abnormal flagella and the decreased motility of *flhF* (T13A), *flhF* (K159A) and *flhF* (G231A), we speculated that the expression of σ54 and σ28-dependent flagella genes would also decrease. Compared with the wild-type strain, the expression of *fliK*, *flgE*, *flhG, flaB and flaA* was significantly reduced in the *flhF* (T13A), *flhF* (K159A) and *flhF* (G231A) by qRT-PCR (Fig. 4B).

We also evaluated the production capacity of proteins encoded by σ54 and σ28-dependent transcripts in the mutant strains. We analyzed the production of FliK, which controls the length of the flagellum, FlhG, which regulates the number of the flagellum, and FlaA, filament protein by western blot (Burnham & Hendrixson, 2018; Klancnik et al., 2019). The results indicated that the production of FliK, FlaA and FlhG were all significantly reduced in *flhF* (T13A), *flhF* (K159A) and *flhF* (G231A) (Fig. 4C). Altogether, the three individual point mutants in B- and N-domains significantly disrupted flagella gene expression and transcription.

4. Discussion

In *C. jejuni*, FlhF is critical for flagellar biosynthesis (Beeby, 2015; Subramanian & Kearns, 2019). Its deletion results in a nonmotile and non-flagellar phenotype. FlhF is a multiple-domain (B-N-G) protein (Gao et al., 2015). However, the role of B- and N-

domains of FlhF in flagella biosynthesis is still unclear in *C. jejuni*. This study showed that both the B- and N-domains were essential for flagellar synthesis. Point mutations in the B- and N-domains induced abnormal flagella assembly. Therefore, we hypothesize that the B- and N-domains may directly regulate flagella synthesis by affecting flagellar gene expression or indirectly influencing GTPase activity. The preliminary investigation of the role of BN- domains in this study can lead to further exploration of the BN domains and their respective functions.

In *B. subtilis*, the B domain regulates and stabilizes the dimer in the presence of GTP, while the N-domain rearranges SRP conformation when the ribosome is bound to stabilize the GTP binding state (Bange et al., 2007; Halic et al., 2006). This study found that *flhF*(T13A), *flhF*(K159A) and *flhF*(G231A) mutants had significant defects in GTPase activity, indicating that the B domain and N domain could influence FlhF binding to GTP, thereby reducing the GTPase activity of FlhF. In addition, FlhF significantly influenced the flagellar gene expression as a global regulator, but the GTPase activity of FlhF was not required for flagellar gene expression in *C. jejuni*. Thus, we speculate that the B- and N-domains of FlhF could play a more important role in the expression of flagellar genes compared to the G-domain.

In *V. cholerae,* the N-domain determines the flagellar polar localization (Green et al., 2009). In *Shewanella oneidensis,* the polarity positioning of FlhF is affected by the B- and N-domains (Gao et al., 2015). This study showed that B- and N-domains also affect the polar targeting of FlhF in *C. jejuni*. So far, no study has shown how B- and N-domains influence flagella biosynthesis in *C. jejuni*. We generated truncated variants of

FlhF with the absent of B- or/and N-domains and found that none of these variants could complemented the flagellar phenotype (Fig. 1), which was also consistent with phenomenon in *B. subtilis* (Gao et al., 2015).

C. jejuni normally generates unipolar or bipolar flagella (Burnham & Hendrixson, 2018; Faber et al., 2016; Matsunami et al., 2016). In our study, various incomplete flagellar phenotypes was observed, including abnormal number and positioning of flagella, or production of a significantly shorter flagellum in -BN domain *flhF* point mutants. It has been known that FlhG can interact with FlhF to control the number of flagella, FliK controls the growth length of flagella (Klancnik et al., 2019). In this study, the gene expression and protein transcription of FlhG and FliK were significantly down-regulated in -BN domain *flhF* point mutants, indicating that abnormal flagella induced by the point mutations in the B- and N-domains had an association with the defects of *flhG* and *fliK* expression.

5. Conclusion

This study initially elucidated the role of the B- and N-domain involved in flagellar synthesis and gene expression in *C. jejuni*. Collectively, our results demonstrated that B- and N-domains might directly or indirectly cause flagella abnormalities by affecting flagellar gene expression or GTPase activity. This study could help us better understand the role of FlhF in flagellar synthesis and lay the basis for FlhF functional research in the future.

Data Availability

All data is within the manuscript and figure.

Author statement

XL, YT, JH conceived and designed the experiments. XL, QC, LZ and PH performed the experiments. XL analyzed the data. XL, JH and XJ contributed reagents, materials, and analysis tools. XL wrote the paper and OG, YT, JH reviewed the manuscript. All authors have read and agreed to the published version of the manuscript.

Declaration of Competing Interest

The authors declare no conflict of interest.

Acknowledgments

This study was supported by the National Natural Science Foundation of China (31872493 and 32172939), Postgraduate Research & Practice Innovation Program of Jiangsu, China (Grant No. SJCX21_1632), and the Priority Academic Program Development of Jiangsu Higher Education Institutions.

Appendix A. Supplementary data

The following is Supplementary data to this article:

Supplementary material related to this article can be found, in the online version, at doi:https://doi.org/10.1016/j.micres.2021.126944.

References

Arroyo-Perez, E. E., & Ringgaard, S. 2021. Interdependent Polar Localization of FlhF and FlhG and Their Importance for Flagellum Formation of *Vibrio parahaemolyticus*. Front Microbiol. 12, 655239. https://dx.doi.org/10.3389/fmicb.2021.655239.

Balaban, M., Joslin, S. N., & Hendrixson, D. R. 2009. FlhF and its GTPase activity are required for distinct processes in flagellar gene regulation and biosynthesis in *Campylobacter jejuni*. J Bacteriol. 191(21), 6602-6611. https://dx.doi.org/10.1128/JB.00884-09.

Bange, G., Petzold, G., Wild, K., & Sinning, I. 2007. Expression, purification and preliminary crystallographic characterization of FlhF from *Bacillus subtilis*. Acta Crystallogr Sect F Struct Biol Cryst Commun. 63(Pt 5), 449-451.

https://dx.doi.org/10.1107/S1744309107020180.
Beeby, M. 2015. Motility in the epsilon-proteobacteria. Curr Opin Microbiol. 28, 115-121. https://dx.doi.org/10.1016/j.mib.2015.09.005.
Burnham, P. M., & Hendrixson, D. R. 2018. *Campylobacter jejuni*: collective components promoting a successful enteric lifestyle. Nat Rev Microbiol. 16(9), 551-565. https://dx.doi.org/10.1038/s41579-018-0037-9.
De Nisco, N. J., Rivera-Cancel, G., & Orth, K. 2018. The Biochemistry of Sensing: Enteric Pathogens Regulate Type III Secretion in Response to Environmental and Host Cues. mBio. 9(1), e02122-02117. https://dx.doi.org/10.1128/mBio.02122-17.
Faber, E., Gripp, E., Maurischat, S., Kaspers, B., Tedin, K., Menz, S., Zuraw, A., Kershaw, O., Yang, I., Rautenschlein, S., & Josenhans, C. 2016. Novel Immunomodulatory Flagellin-Like Protein FlaC in *Campylobacter jejuni* and Other Campylobacterales. mSphere. 1(1), e00028-00015. https://dx.doi.org/10.1128/mSphere.00028-15.
Ferreira, J. L., Coleman, I., Addison, M. L., Zachs, T., Quigley, B. L., Wuichet, K., & Beeby, M. 2021. The "Jack-of-all-Trades" Flagellum From *Salmonella* and *E. coli* Was Horizontally Acquired From an Ancestral beta-Proteobacterium. Front Microbiol. 12, 643180. https://dx.doi.org/10.3389/fmicb.2021.643180.
Gao, T., Shi, M., Ju, L., & Gao, H. 2015. Investigation into FlhFG reveals distinct features of FlhF in regulating flagellum polarity in *Shewanella oneidensis*. Mol Microbiol. 98(3), 571-585. https://dx.doi.org/10.1111/mmi.13141.
Green, J. C., Kahramanoglou, C., Rahman, A., Pender, A. M., Charbonnel, N., & Fraser, G. M. 2009. Recruitment of the earliest component of the bacterial flagellum to the old cell division pole by a membrane-associated signal recognition particle family GTP-binding protein. J Mol Biol. 391(4), 679-690. https://dx.doi.org/10.1016/j.jmb.2009.05.075.
Gulbronson, C. J., Ribardo, D. A., Balaban, M., Knauer, C., Bange, G., & Hendrixson, D. R. 2016. FlhG employs diverse intrinsic domains and influences FlhF GTPase activity to numerically regulate polar flagellar biogenesis in *Campylobacter jejuni*. Mol Microbiol. 99(2), 291-306. https://dx.doi.org/10.1111/mmi.13231.
Gundogdu, O., da Silva, D. T., Mohammad, B., Elmi, A., Wren, B. W., van Vliet, A. H., & Dorrell, N. 2016. The *Campylobacter jejuni* Oxidative Stress Regulator RrpB Is Associated with a Genomic Hypervariable Region and Altered Oxidative Stress Resistance. Front Microbiol. 7, 2117. https://dx.doi.org/10.3389/fmicb.2016.02117.
Gundogdu, O., Mills, D. C., Elmi, A., Martin, M. J., Wren, B. W., & Dorrell, N. 2011. The *Campylobacter jejuni* transcriptional regulator Cj1556 plays a role in the oxidative and aerobic stress response and is important for bacterial survival in vivo. J Bacteriol. 193(16), 4238-4249. https://dx.doi.org/10.1128/JB.05189-11.
Halic, M., Blau, M., Becker, T., Mielke, T., Pool, M. R., Wild, K., Sinning, I., & Beckmann, R. 2006. Following the signal sequence from ribosomal tunnel exit to signal recognition particle. Nature. 444(7118), 507-511.

https://dx.doi.org/10.1038/nature05326.
Han, D., Xu, L., Liu, P., Liu, Y., Sun, C., & Yin, Y. 2019. Allicin disrupts cardiac Cav1.2 channels via trafficking. Pharm Biol. 57(1), 245-249. https://dx.doi.org/10.1080/13880209.2019.1577469.
Jervis, A. J., Butler, J. A., Wren, B. W., & Linton, D. 2015. Chromosomal integration vectors allowing flexible expression of foreign genes in *Campylobacter jejuni*. BMC Microbiol. 15, 230. https://dx.doi.org/10.1186/s12866-015-0559-5.
Kazmierczak, B. I., & Hendrixson, D. R. 2013. Spatial and numerical regulation of flagellar biosynthesis in polarly flagellated bacteria. Mol Microbiol. 88(4), 655-663. https://dx.doi.org/10.1111/mmi.12221.
Klancnik, A., Simunovic, K., Kovac, J., Sahin, O., Wu, Z., Vuckovic, D., Abram, M., Zhang, Q., & Mozina, S. S. 2019. The Anti-*Campylobacter* Activity and Mechanisms of Pinocembrin Action. Microorganisms. 7(12), 675. https://dx.doi.org/10.3390/microorganisms7120675.
Kojima, S., Terashima, H., & Homma, M. 2020. Regulation of the Single Polar Flagellar Biogenesis. Biomolecules. 10(4), 533. https://dx.doi.org/10.3390/biom10040533.
Kondo, S., Homma, M., & Kojima, S. 2017. Analysis of the GTPase motif of FlhF in the control of the number and location of polar flagella in *Vibrio alginolyticus*. Biophys Physicobiol. 14, 173-181. https://dx.doi.org/10.2142/biophysico.14.0_173.
Kulshreshtha, P., Tiwari, A., Priyanka, Joon, S., Sinha, S., & Bhatnagar, R. 2015. Investigation of a panel of monoclonal antibodies and polyclonal sera against anthrax toxins resulted in identification of an anti-lethal factor antibody with disease-enhancing characteristics. Mol Immunol. 68(2 Pt A), 185-193. https://dx.doi.org/10.1016/j.molimm.2015.07.019.
Li, X., Ren, F., Cai, G., Huang, P., Chai, Q., Gundogdu, O., Jiao, X., & Huang, J. 2020. Investigating the Role of FlhF Identifies Novel Interactions With Genes Involved in Flagellar Synthesis in *Campylobacter jejuni*. Front Microbiol. 11, 460. https://dx.doi.org/10.3389/fmicb.2020.00460.
Li, M., Zhu, X., Zhao, B., Shi, L., Wang, W., Hu, W., Qin, L., Chen, B., Zhou, P., Qiu, B., Gao, Y., & Liu, B. 2019. Adrenomedullin alleviates the pyroptosis of Leydig cells by promoting autophagy via the ROS-AMPK-mTOR axis. Cell Death Dis. 10(7), 489. https://dx.doi.org/10.1038/s41419-019-1728-5.
Liang, L., & Connerton, I. F. 2018. FlhF(T368A) modulates motility in the bacteriophage carrier state of *Campylobacter jejuni*. Mol Microbiol. 110(4), 616-633. https://dx.doi.org/10.1111/mmi.14120.
Matsunami, H., Barker, C. S., Yoon, Y. H., Wolf, M., & Samatey, F. A. 2016. Complete structure of the bacterial flagellar hook reveals extensive set of stabilizing interactions. Nat Commun. 7, 13425. https://dx.doi.org/10.1038/ncomms13425.
Mazzantini, D., Fonnesu, R., Celandroni, F., Calvigioni, M., Vecchione, A., Mrusek, D., Bange, G., & Ghelardi, E. 2020. GTP-Dependent FlhF Homodimer Supports Secretion of a Hemolysin in *Bacillus cereus*. Front Microbiol. 11,

879. https://dx.doi.org/10.3389/fmicb.2020.00879.
Ren, F., Lei, T., Song, Z., Yu, T., Li, Q., Huang, J., & Jiao, X. A. 2018. Could FlhF be a key element that controls *Campylobacter jejuni* flagella biosynthesis in the initial assembly stage? Microbiol Res. 207, 240-248. https://dx.doi.org/10.1016/j.micres.2017.12.006.
Schniederberend, M., Abdurachim, K., Murray, T. S., & Kazmierczak, B. I. 2013. The GTPase activity of FlhF is dispensable for flagellar localization, but not motility, in *Pseudomonas aeruginosa*. J Bacteriol. 195(5), 1051-1060. https://dx.doi.org/10.1128/JB.02013-12.
Schuhmacher, J. S., Thormann, K. M., & Bange, G. 2015. How bacteria maintain location and number of flagella? FEMS Microbiol Rev. 39(6), 812-822. https://dx.doi.org/10.1093/femsre/fuv034.
Subramanian, S., & Kearns, D. B. 2019. Functional Regulators of Bacterial Flagella. Annu Rev Microbiol. 73, 225-246. https://dx.doi.org/10.1146/annurev-micro-020518-115725.
Terashima, H., Hirano, K., Inoue, Y., Tokano, T., Kawamoto, A., Kato, T., Yamaguchi, E., Namba, K., Uchihashi, T., Kojima, S., & Homma, M. 2020. Assembly Mechanism of a Supramolecular MS-Ring Complex To Initiate Bacterial Flagellar Biogenesis in *Vibrio* Species. J Bacteriol. 202(16), e00236-00220.
Zhang, K., He, J., Cantalano, C., Guo, Y., Liu, J., & Li, C. 2020. FlhF regulates the number and configuration of periplasmic flagella in *Borrelia burgdorferi*. Mol Microbiol. 113(6), 1122-1139. https://dx.doi.org/10.1111/mmi.14482.

445 **Table 1** Number and position of flagella in wild-type and mutant strains

Relevant genotype[a]	% of bacteria with[b]			
	2 flagella	1 flagellum	0 flagella	Other forms
WT	78	13	9	0
△*flhF*	0	0	100	0
T13A	1	9	61	29
K159A	3	9	51	37
G231A	4	11	47	38

446 [a] Strains used include WT (wild-type 81-176), T13A [*flhF* (T13A)], K159A [*flhF*
447 (K159A)], G231A [*flhF* (G231A)].

448 [b] The percentage of each phenotype among the 100 bacteria in the strain. Phenotypes
449 included unipolar, bipolar flagella, or without flagella. The abnormal flagella phenotype
450 included producing multiple flagella in a unipolar position, a sharply shortened flagella
451 or one flagella in a non-polar or lateral position.
452

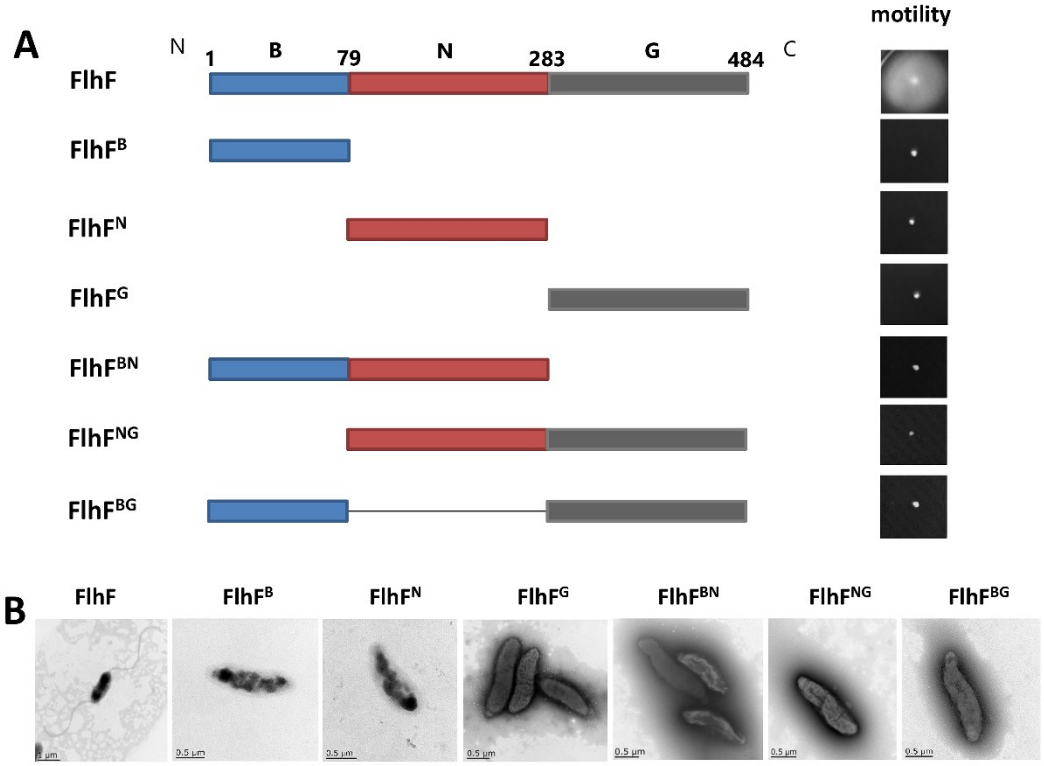

453

454 **Fig. 1. Role of B- and N-domains for the motility and flagellar biosynthesis.**

455 (A) FlhF variants in *C. jejuni*. B-region (blue box; residues 1-78); N-region (red box;
456 residues 79-272); and G-region (black box; residues 283-484). FlhF^{B} (residues 1-78),
457 FlhF^{N} (residues 79-272), FlhF^{G} (residues 283-484), FlhF^{BN} (residues 1-272), FlhF^{NG}
458 (residues 79-484), and FlhF^{BG} (residues 79-272 deleted). In motility assays, cells were
459 spotted in MH semi-solid agar and incubated at 42°C. (B) TEM visualization of wild-
460 type (WT) and *flhF* mutants. All results were from representatives of three independent
461 experiments.

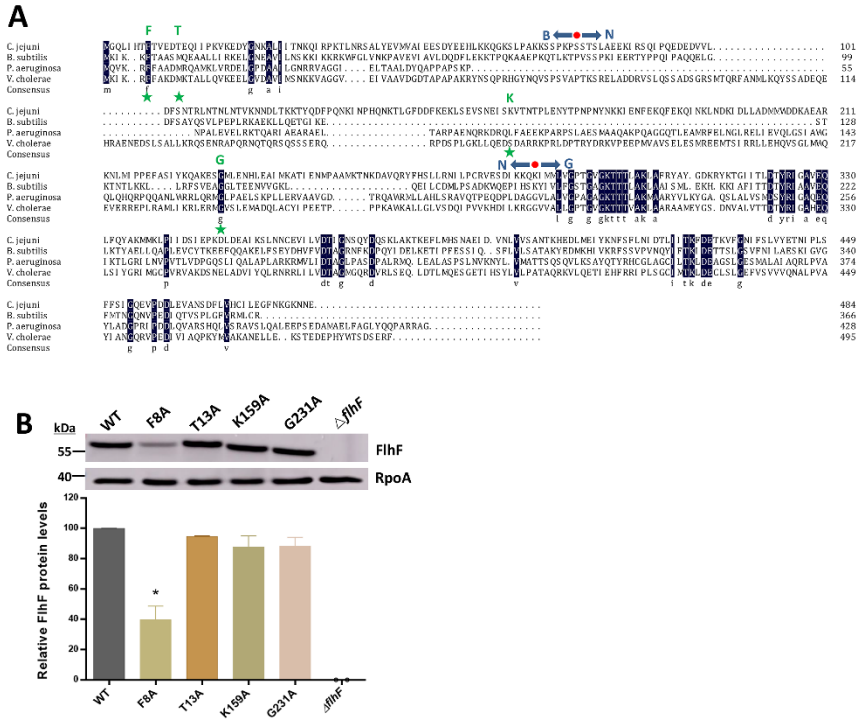

462

463 **Fig. 2. Point mutants in the BN-domains and immunoblot analysis of FlhF**
464 **production.**

465 (A) The sequence alignment of the FlhF of *C. jejuni*, *B. subtilis* FlhF, *P. aeruginosa*
466 FlhF and *V. cholerae* FlhF. Black represents 100% similarity of residues. Green
467 asterisks indicated residues in *C. jejuni* FlhF substituted for alanine, including F8A,
468 T13A in B domain, and K159A, G231A in N-domain. (B) Western blot analysis of
469 wild-type and FlhF mutant proteins in *C. jejuni*. The mouse anti-FlhF antiserum was
470 used to detect FlhF protein from WCL, and mouse anti-RpoA antiserum was used to
471 detect RpoA in WCL. Strains include wild-type 81-176, *flhF* (F8A), *flhF* (T13A), *flhF*
472 (K159A), *flhF* (G231A) strains. All results were from representatives of three
473 independent experiments. Compared to the average WT value set as 100%, the data was
474 quantified and the error bars represented the standard deviation of independent
475 replicates. The data was analyzed using Student's *t*-test (*P<0.05, **P<0.01,
476 ***P<0.001).

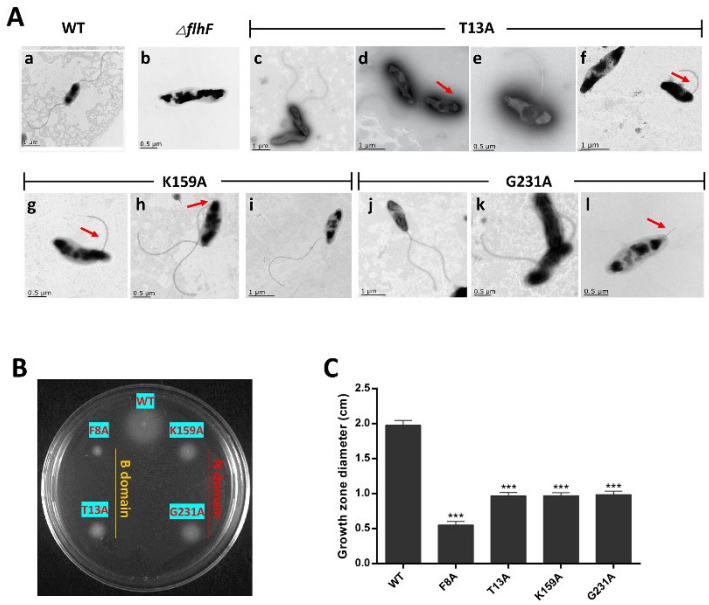

477

478 **Fig. 3. Analysis of flagellar phenotypes and motility of WT and *flhF* mutant strains.**

479 (A) The flagellar phenotypes of *C. jejuni* of wild-type and *flhF* mutants. (a) Wide type;

480 (b) *△flhF* mutant strain; (c to f) *flhF* (T13A) mutant strain; (g to i) *flhF* (K159A) mutant

481 strain; (j to l) *flhF* (G231A) mutant strain. The red arrows represented the truncated

482 flagella produced in d, f, g, h and l. (B) Motility phenotypes of wild-type and *flhF* point

483 mutant strains including *flhF* (F8A), *flhF* (T13A), *flhF* (K159A), *flhF* (G231A) strains.

484 (C) Diameter of wild-type and *flhF* point mutant strains including *flhF* (F8A), *flhF*

485 (T13A), *flhF* (K159A), *flhF* (G231A) strains on semisolid agar plates. Significance was

486 tested by Student's *t*-test (*** represented significance at $P < 0.001$).

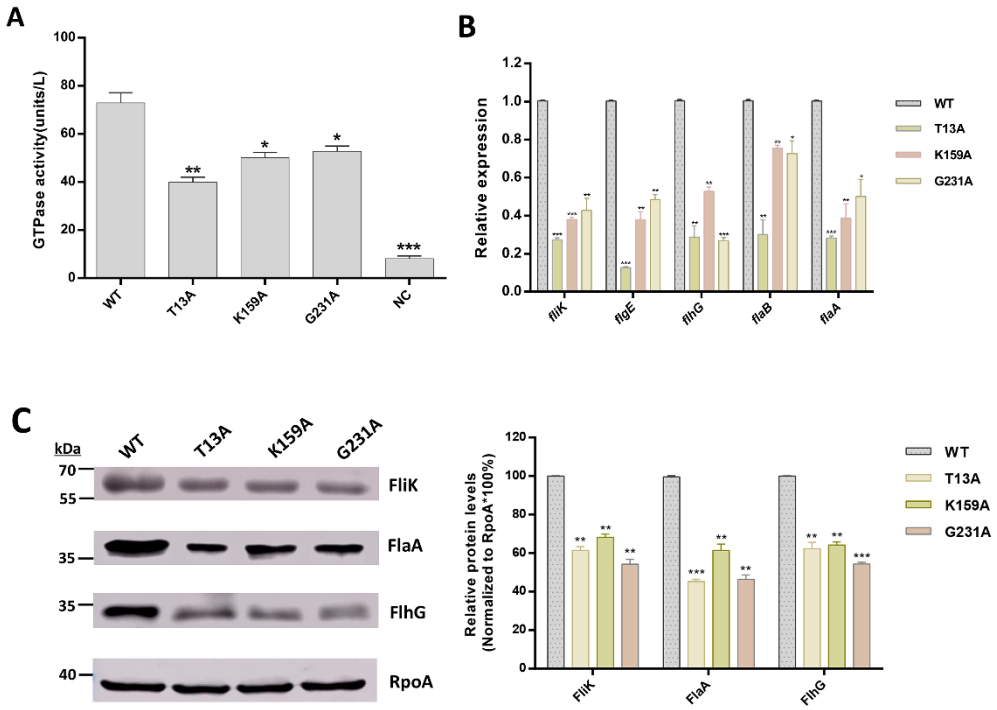

Fig. 4. Analysis of GTPase activity, flagella gene expression and protein transcript of WT and *flhF* mutant strains.

(A) GTPase activity of WT and FlhF point mutants, including *flhF* (T13A), *flhF* (K159A), *flhF* (G231A) strains**.** NC represented Negative control. (B) Analysis of flagellar gene expression in the *flhF* mutant by qRT-PCR, including *fliK*, *flgE*, *flhG*, *flab* and *flaA*. The *glyA* gene was set as an endogenous control. The relative gene expression of wild-type was set as 1. (C) Western blot analysis of wild-type and FlhF mutant proteins in *C. jejuni*. The mouse anti-FliK, FlhG and RpoA antiserum were used to detect FliK, FlhG and RpoA protein from WCL, respectively. Mouse anti-RpoA antiserum was used to detect RpoA in WCL. Wild-type 81-176 (WT), *flhF* (F8A), *flhF* (T13A), *flhF* (K159A), *flhF* (G231A) strains were used. Compared to the average WT value set at 100%, the data was quantified and the error bars represented the standard deviation of independent replicates. All results were from representatives of three independent experiments. Data were analyzed using Student's *t*-test (*P<0.05, **P<0.01, ***P<0.001).